Charge Transfer Complexes Based on the Twin-TCNQ-Type Acceptor 11,11,12,12,13,13,14,14-Octacyano-1,4:5,8-anthradiquinotetramethane (OCNAQ)

Tamotsu INABE,* Tsutomu MITSUHASHI,[†] and Yusei MARUYAMA*

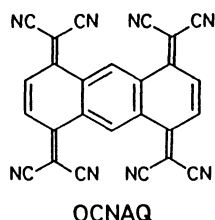Institute for Molecular Science, Myodaiji, Okazaki 444

[†]Department of Chemistry, Faculty of Science, The University of Tokyo, Bunkyo-ku, Tokyo 113

(Received May 13, 1988)

Charge transfer complexes of OCNAQ with pyrene, PT (phenothiazine), TMTTF (tetramethyltetrathiafulvalene), TTT (5,6:11,12-bis(epidithio)naphthacene), and TTF (tetrathiafulvalene) have been prepared. The pyrene and PT complexes are electrically insulating and the ground state is neutral. In most of the other complexes OCNAQ is fully charged. One of the TTT complexes, (TTT)$_2$OCNAQ(DMF), where DMF is N,N-dimethylformamide, has been found to show metallic conductivity. A structural study has revealed that short S···N contacts exist between TTT and OCNAQ, in addition to one-dimensional TTT stacks. This transverse interaction has been demonstrated by the small anisotropy of the conductivity. The 2:1 TTF complex is also metallic down to 43 K, at which point a metal-to-insulator transition occurs. A structure analysis and thermoelectric power data suggest that the charge conduction in this crystal takes place not only through the TTF stacks but also through a two-dimensional network of the OCNAQ molecules.
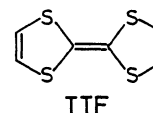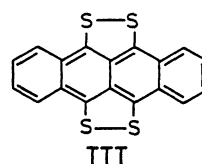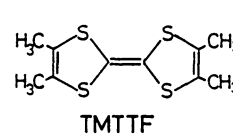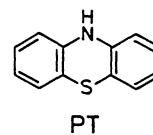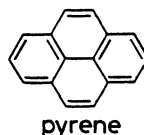
Recently, a synthesis and characterization of the title compound OCNAQ (systematic name: 1,4,5,8-tetrakis-(dicyanomethylene)anthracene), a twin-TCNQ-type acceptor, has been reported.[1,2] From its molecular structure it is expected that the on-site Coulomb repul-

OCNAQ

sion should be reduced compared with TCNQ. In fact, a cyclic voltammogram shows that the first and second redox waves are closely located.[1,2] Furthermore, the monovalent tetraethylammonium salt Et$_4$N·OCNAQ exhibits a rather high conductivity[2] as a simple salt. The molecular shape of OCNAQ is nonplanar due to a steric interaction between the cyano groups. The nonplanarity is not advantageous for high electrical conduction through the molecular stacks, since insufficient overlapping between the molecules in a stack causes a small transfer integral and, consequently, a partial reduction state cannot be sufficiently stabilized. Actually, the approaches to obtain any fractionally reduced OCNAQ salts with closed-shell cationic species have so far failed, and only monoanionic and dianionic OCNAQ salts have been obtained.

As a next step toward achieving higher conductivity based on OCNAQ, complexes with various donor molecules, instead of closed-shell cationic species, have been investigated, and the metallic properties of (TTT)$_2$OCNAQ(DMF) have recently been reported.[3] In this compound OCNAQ interacts transversely with the TTT stacks. In this paper the preparation, structures, and charge transport properties of the OCNAQ complexes with pyrene, PT, TMTTF, TTT, and TTF

are described. Among them, one of the TTF complexes has been found to be metallic, in which the OCNAQ molecules form a two-dimensional network. A twin-type molecular structure may be responsible for this stacking nature.

pyrene   PT   TMTTF

TTT   TTF

Experimental

Materials. OCNAQ was synthesized by the same method reported previously.[2] DMF used as a solvent was dried with Molecular Sieve 4A and distilled under reduced pressure. Acetonitrile was dried before distillation with P$_2$O$_5$ and repeated with K$_2$CO$_3$. 1,2-Dichlorobenzene was used without purification. All donors were purified by recrystallization or sublimation.

Pyrene–OCNAQ: Slow cooling of a hot acetonitrile solution containing pyrene and OCNAQ with a molar ratio of 3:1 yielded black needle-like crystals. Solvent inclusion was found by elemental analysis. Found: C, 78.48; H, 2.79; N, 18.57%. Calcd for C$_{44}$H$_{19}$N$_9$ (pyrene·OCNAQ(CH$_3$CN)): C, 78.45; H, 2.84; N, 18.70%.

PT–OCNAQ: The complex was prepared by slow cooling of a hot acetonitrile solution, including PT and OCNAQ, with a molar ratio of 4:1. The precipitate was found to be a mixture of two kinds of crystals; one is a black needle-like crystal and another is a brown plate-like crystal. One polymorph is PT·OCNAQ(CH$_3$CN) and the other is PT·OCNAQ. Found: C, 72.06; H, 2.46; N, 20.21%. Calcd

for 2:3 weight fraction of PT·OCNAQ and PT·OCNAQ-(CH_3CN): C, 71.98; H, 2.59; N, 20.53%.

TMTTF-OCNAQ: A powdered material was prepared by mixing TMTTF in hot acetonitrile and OCNAQ in the same solvent with a molar ratio of 2:1. The elemental analysis indicated the 1:1 stoichiometry. Found: C, 62.48; H, 2.68; N, 16.30%. Calcd for $C_{36}H_{18}N_8S_4$: C, 62.59; H, 2.63; N, 16.21%. The same material was obtained in a fine needle-like shape by conventional electrocrystallization using $Et_4N·OCNAQ$ as a supporting electrolyte.

TTT-OCNAQ: Slow cooling of a hot 1,2-dichloroben-zene solution containing TTT and OCNAQ with a molar ratio of 1:1 gave black plate-like crystals. An elemental analysis shows that the composition is $(TTT)_3(OCNAQ)_2$-$(dichlorobenzene)_2$, abbreviated TTT-OCNAQ(I). Found: C, 64.26; H, 1.85; N, 10.40; S, 17.21%. Calcd for $C_{94}H_{44}$-$Cl_4N_{16}S_{12}$: C, 64.06; H, 2.19, N, 10.13; S, 17.40%.

When the complex was prepared electrochemically in DMF, the obtained crystal was found to contain DMF molecules. The composition confirmed by an X-ray structure analysis was $(TTT)_2OCNAQ(DMF)$, abbreviated TTT-OCNAQ(II).

TTF-OCNAQ: The complexes were prepared by the following three methods: (1) mixing of the TTF and OCNAQ solutions, and (2) mixing of the $(TTF)_3(BF_4)_2$ and $Et_4N·$OCNAQ solutions, (3) electrocrystallization. Acetonitril was used as a solvent. Microcrystals were obtained by the first and second methods. An elemental analysis of these materials always showed a slight deviation from the 1:1 stoichiometry, i.e., an excess content of TTF.[1] This small deviation is due to the coexistence of a 1:1 phase and a donor-rich phase. In fact, the stoichiometry of the minor product obtained by the third method was found to be 2:1 by X-ray structure analysis. The correspondence of the major products in all methods was confirmed by optical and electrical measurements. Hereafter, the 1:1 complex is abbreviated TTF-OCNAQ(I) and the 2:1 complex TTF-OCNAQ(II).

Measurements. Infrared spectra were taken by a HITA-CHI 295 spectrometer by using a Nujol mull specimen. Electrical conductivity measurements were carried out by a conventional four-probe or two-probe method. Thermo-electric power measurements were performed by a method similar to that reported by Chaikin and Kwak.[4]

X-Ray Structure Analyses. The computer program system used was UNICSIII[5] run on a HITACHI M680 at IMS.**

TTT-OCNAQ(II): A black plate-like crystal having approximate dimensions of $0.40×0.15×0.05$ mm^3 was used for the crystallographic study. Diffraction data were collected at room temperature using an automated RIGAKU AFC-5R fourcircle diffractometer with graphite mono-chromatized Mo $K\alpha$ radiation. Fifty reflections with $20°<\theta<30°$ were used to determine the lattice parameters. Crystal data; chemical formula $C_{65}H_{29}N_9OS_8$, formula weight $M=1208.51$, triclinic, space group $P\bar{1}$, $a=11.522(2)$, $b=16.406(3)$, $c=7.942(1)$ Å, $\alpha=94.23(2)$, $\beta=95.13(2)$, $\gamma=116.51(1)°$, $V=1327.0(4)$ Å^3, $Z=1$, $D_c=1.51$ g cm^{-3}, and $\mu=3.77$ cm^{-1}. The intensity data were collected in the region $2\theta<60°$ in the θ-2θ mode at a scan rate of $6°$ min^{-1}. 3716 independent reflections with $|F_o|>3\sigma(F_o)$ were used for a structure analysis. The structure was solved by the Patterson method. An aniso-tropic block-diagonal least-squares refinement for non-

** IMS: Institute for Molecular Science.

hydrogen atoms with isotropic hydrogen atoms gave a final R value of 0.063.

TTF-OCNAQ(III): A black plate-like crystal having approximate dimensions of $0.33×0.15×0.05$ mm^3 was used for the crystallographic study. The data collection and structure analysis were performed using the same procedure as TTF-OCNAQ(II), except for the diffractometer (RIGAKU AFC-5) and scan rate $(3° min^{-1})$. Crystal data; chemical formula $C_{38}H_{14}N_8S_8$, formula weight $M=839.04$, triclinic, space group $P\bar{1}$, $a=6.702(6)$, $b=19.302(8)$, $c=7.239(5)$ Å, $\alpha=86.69(5)$, $\beta=109.22(8)$, $\gamma=93.64(6)°$, $V=882(1)$ Å^3, $Z=1$, $D_c=1.58$ g cm^{-3} and $\mu=5.29$ cm^{-1} The intensiy data were collected in the region $2\theta<50°$; 1126 independent reflections with $|F_o|>3\sigma(F_o)$ were used for a structure analysis. The final R value was 0.061.

Results and Discussion

Infrared Spectra. Chapell et al. showed that the reduction state of TCNQ could be estimated from the frequency of the C≡N stretching mode.[6] For OCNAQ, a similar dependence of the frequency of the C≡N stretching mode on the reduction state is expected, since the same type LUMO as TCNQ was obtained by calculation.[2] Figure 1 shows the C≡N stretching bands for OCNAQ, $Et_4N·OCNAQ$, and $(Et_4N)_2$-OCNAQ. The frequency is 2214, 2186, and 2170 cm^{-1}, respectively; thus, a similar charge dependence of the frequency can be obtained. However, the frequency
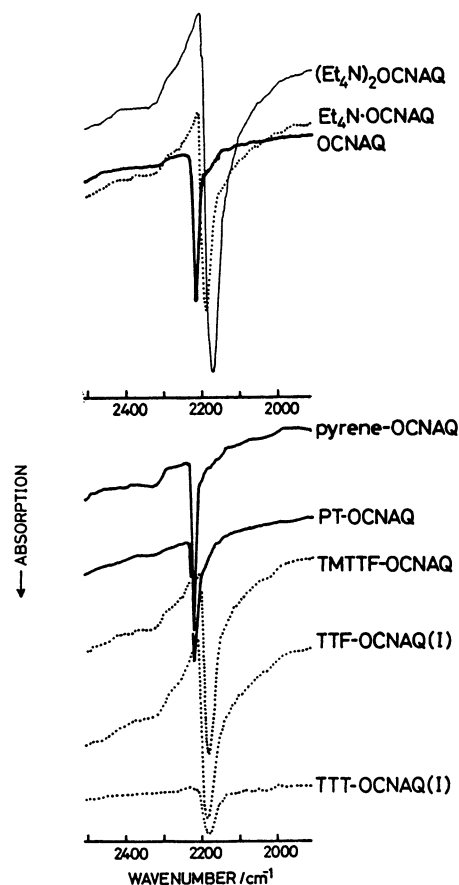

Fig. 1. Infrared spectra of OCNAQ and the OCNAQ complexes.

shift by charge is not as large as that of TCNQ (frequency shift $\Delta\nu$ for TCNQ$\rightarrow$TCNQ$^-$, 44 cm^{-1}; $\Delta\nu$ for OCNAQ$\rightarrow$OCNAQ$^-$, 28 cm^{-1}). This seems to arise from the main characteristics of OCNAQ, namely a twin-TCNQ-type nature. Indeed, the shift from OCNAQ to OCNAQ^{2-} amounts to 44 cm^{-1}, which is exactly the same as that from TCNQ to TCNQ$^-$.

The C≡N stretching bands in the infrared spectra for pyrene-OCNAQ, PT-OCNAQ, TMTTF-OCNAQ, TTF-OCNAQ(I), and TTT-OCNAQ(I) are also shown in Fig. 1. Owing to an electronic transition, which extends in this region in TTT-OCNAQ(II), the infrared spectrum did not provide any useful information about the ionicity of this compound. Data for TTF-OCNAQ(II) are also absent, because the sample amount was insufficient to examine the infrared spectrum. From the position of the C≡N stretching mode a neutral nature was found for the pyrene and PT complexes. Since the ionization potentials of pyrene and PT are relatively high compared with the other donor molecules, a neutral nature for the ground state is reasonable. In the other complexes the OCNAQ molecules are fully ionized, and the electronic structures are represented as (TMTTF$^+$)(OCNAQ$^-$), (TTF$^+$)-(OCNAQ$^-$) for TTF-OCNAQ(I), and (TTT$_3$)$^{2+}$-(OCNAQ$^-$)$_2$(dichlorobenzene)$_2$ for TTT-OCNAQ(I).

Crystal Structure. TTT-OCNAQ(II): The molecular structures of TTT and OCNAQ in this compound, obtained by X-ray analysis, are shown in Fig. 2 and the atomic parameters are listed in Table 1.[7] The TTT molecule is essentially planar (deviations from the mean plane are less than 0.15 Å for non-hydrogen atoms). On the other hand, the OCNAQ molecule is largely deformed from the planar structure. The deformation pattern is the same as that observed in
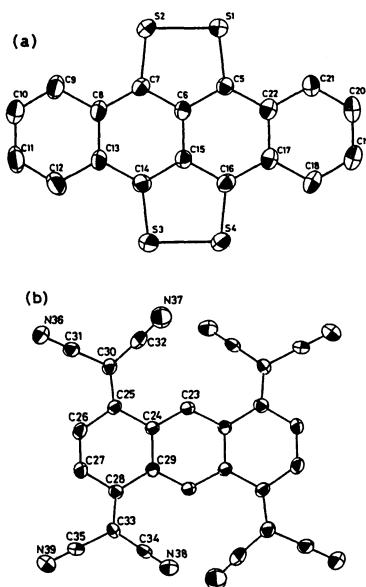

Fig. 2. ORTEP drawing[15] of TTT (a) and OCNAQ (b) in TTT-OCNAQ(II) showing the atom numbering scheme.
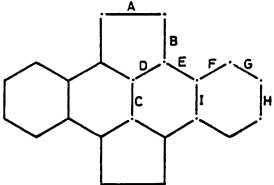
Table 1. Atomic Parameters of TTT-OCNAQ(II) ($\times 10^4$)

	x	y	z	$B_{eq}/\text{Å}^2$
S1	2245(2)	2234(1)	4723(3)	3.0
S2	1200(2)	2800(1)	3424(3)	3.2
S3	−2816(2)	−1120(1)	−153(3)	3.4
S4	−1754(2)	−1681(1)	1132(3)	3.3
C5	1313(7)	1129(5)	3726(9)	2.2
C6	239(7)	1018(5)	2577(9)	2.2
C7	49(8)	1781(5)	2261(10)	2.3
C8	−1035(8)	1680(5)	1108(10)	2.6
C9	−1203(9)	2466(6)	720(11)	3.5
C10	−2292(9)	2334(6)	−356(12)	3.9
C11	−3217(9)	1459(7)	−1069(12)	4.1
C12	−3087(9)	690(8)	−745(11)	3.5
C13	−1979(8)	784(5)	336(10)	2.4
C14	−1772(8)	16(5)	685(10)	2.4
C15	−667(7)	127(5)	1769(10)	2.3
C16	−498(8)	−643(5)	2121(10)	2.4
C17	601(8)	−545(5)	3242(10)	2.4
C18	811(8)	−1314(5)	3590(10)	2.9
C19	1875(9)	−1191(6)	4691(11)	3.3
C20	2780(9)	−305(6)	5475(11)	3.4
C21	2622(8)	456(6)	5189(11)	2.9
C22	1528(8)	366(5)	4053(10)	2.4
C23	−4335(7)	−5362(5)	−4043(9)	2.2
C24	−4453(7)	−4624(5)	−3274(9)	1.9
C25	−3992(7)	−4277(5)	−1481(9)	2.1
C26	−4520(8)	−3710(5)	−737(9)	2.4
C27	−5140(8)	−3333(5)	−1693(9)	2.4
C28	−5312(7)	−3476(5)	−3517(9)	2.0
C29	−5138(7)	−4237(5)	−4271(9)	1.9
C30	−3097(8)	−4446(5)	−440(10)	2.5
C31	−2796(8)	−4116(5)	1332(10)	2.7
C32	−2359(9)	−4888(7)	−964(11)	4.1
C33	−5561(7)	−2866(5)	−4432(9)	2.2
C34	−5463(8)	−2801(5)	−6182(10)	2.6
C35	−5696(8)	−2132(6)	−3575(10)	2.8
N36	−2534(8)	−3858(5)	2759(9)	4.2
N37	−1732(10)	−5226(8)	−1307(12)	7.6
N38	−5325(8)	−2706(5)	−7578(9)	3.9
N39	−5747(9)	−1508(5)	−2904(10)	4.5
N40	−9861(24)	−4726(12)	−5110(38)	5.5
C41	−9006(16)	−4663(13)	−3833(25)	12.6
C42	−9511(24)	−4032(17)	−5799(40)	8.3
O43	−8525(23)	−3338(14)	−5280(34)	12.0

Et$_4$N·OCNAQ,[2] namely the TCNQ nuclei are distorted into boat forms and the two TCNQ boats are linked by two methylidine groups upside-down with each other.
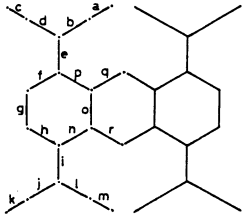
Since the electronic structure cannot be determined by the infrared spectra, the bond lengths of the molecules were carefully examined by X-ray structure analysis in order to elucidate the charge on the molecules. The mean dimensions of TTT are listed in Table 2 along with data for TTT^0, TTT$^{1/2+}$ (TTT$_2$I$_3$), and TTT$^+$ (TTT(TCNQ)$_2$). Major structural differences between TTT^0 and TTT$^{1/2+}$ appear in the bond lengths of A, B, E, and F in Table 2, whereas those between TTT$^{1/2+}$ and TTT$^+$ appear in bond C. By a comparison with these data it is favorable to assign the TTT molecule in TTT-OCNAQ(II) to TTT$^{1/2+}$. The same kind of information can be obtained from the molecular structure of OCNAQ, of which bond

Table 2.   Mean Dimensions of TTT (Å)

	TTT[a]	TTT$_2$I$_3$[a]	TTT-(TCNQ)$_2$[a]	TTT-OCNAQ(II)
A	2.100(2)	2.078(2)	2.082(2)	2.074(4)
B	1.781(6)	1.738(3)	1.732(7)	1.731(10)
C	1.422(13)	1.429(8)	1.375(15)	1.420(9)
D	1.406(7)	1.390(4)	1.401(8)	1.403(13)
E	1.374(7)	1.414(4)	1.431(8)	1.421(12)
F	1.450(7)	1.410(5)	1.426(8)	1.427(14)
G	1.367(7)	1.358(5)	1.360(8)	1.372(15)
H	1.421(11)	1.404(8)	1.401(12)	1.398(12)
I	1.455(9)	1.444(6)	1.413(12)	1.439(11)

a) After Smith and Luth;[8] originally Ref. 9 for TTT and Ref. 10 for TTT(TCNQ)$_2$

Table 3.   Bond Lengths of OCNAQ (Å)

	Et$_4$N·OCNAQ[a]	(Et$_4$N)$_2$-OCNAQ	TTT-OCNAQ(II)	TTF-OCNAQ(II)
a	1.146(15)	1.144(17)	1.130(19)	1.148(15)
b	1.423(15)	1.420(17)	1.411(16)	1.402(15)
c	1.141(13)	1.130(15)	1.144(10)	1.140(15)
d	1.441(19)	1.394(16)	1.423(11)	1.439(15)
e	1.398(11)	1.433(14)	1.401(13)	1.406(15)
f	1.425(15)	1.430(14)	1.440(14)	1.430(14)
g	1.333(13)	1.368(13)	1.354(13)	1.362(15)
h	1.436(13)	1.402(15)	1.432(10)	1.415(15)
i	1.388(11)	1.443(11)	1.392(13)	1.406(15)
j	1.435(14)	1.433(18)	1.416(13)	1.415(15)
k	1.144(15)	1.157(19)	1.146(14)	1.138(15)
l	1.420(14)	1.374(14)	1.413(11)	1.425(18)
m	1.143(13)	1.157(14)	1.146(11)	1.149(17)
n	1.459(13)	1.458(15)	1.445(12)	1.472(14)
o	1.429(11)	1.472(13)	1.436(12)	1.440(14)
p	1.464(12)	1.400(17)	1.452(10)	1.441(13)
q	1.391(13)	1.389(18)	1.384(12)	1.410(14)
r	1.404(13)	1.351(21)	1.400(9)	1.371(14)

a) Averaged values.

lengths are listed in Table 3. Unfortunately, the structure of neutral OCNAQ has not been obtained. However, the molecular dimensions of OCNAQ$^-$ and OCNAQ^{2-} are known[2] and are listed in Table 3. The differences between OCNAQ$^-$ and OCNAQ^{2-} appear in the C=C bond length between dicyanomethylene and the ring carbon (e and i in Table 3). Judging from these bond lengths the charge of OCNAQ in TTT-OCNAQ(II) has been assigned as -1. This assignment

is consistent with the charge of TTT, and the electronic structure of this compound is represented as $(TTT)_{\frac{1}{2}}^+ OCNAQ^-(DMF)$.

The crystal structure is shown in Fig. 3. The TTT molecules form one-dimensional columns along the c-axis, while the OCNAQ molecules overlap only partly with each other. The DMF molecule is positionally disordered, i.e., one DMF molecule can occupy two positions which are related to each other by an inversion center. Molecular overlapping patterns between the TTT molecules in the stack and between the OCNAQ molecules are shown in Fig. 4. The interplanar and short interatomic distances between the molecules are listed in Table 4. There are
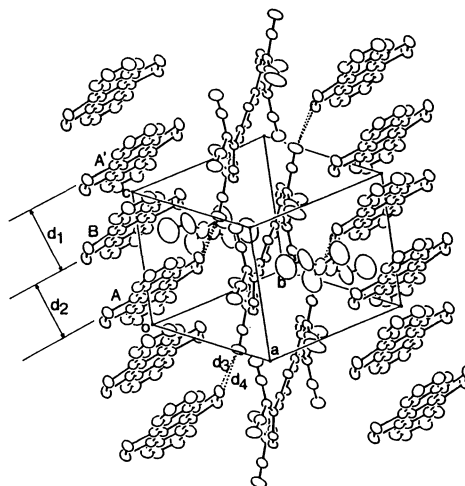

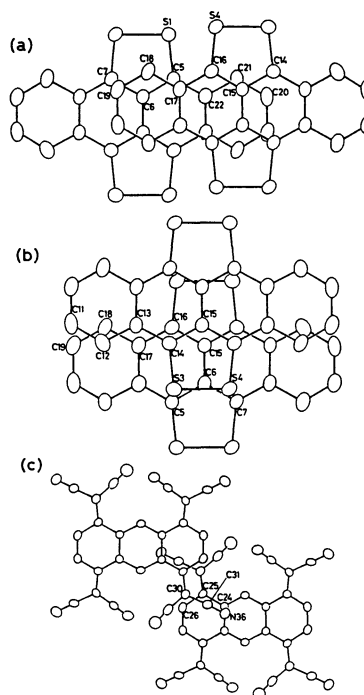Fig. 3.   Crystal structure of TTT–OCNAQ(II).

Fig. 4.   Molecular overlapping between the TTT molecules; between A and B (a), and between B and A' (b) in Fig. 3, and between the OCNAQ molecules (c).

Table 4.   Interplanar and Interatomic Distances (Å) of TTT-OCNAQ(II): between A and B (a) and between B and A' (b) in Fig. 4, between the OCNAQ Molecules (c), and Distances Shown in Fig. 3 (d)

(a)	S1–S4	3.506(3)
	S1–C18	3.587(9)
	C5–C17	3.315(11)
	C6–C18	3.454(12)
	C7–C19	3.332(13)
	C14–C20	3.433(13)
	C15–C21	3.349(12)
	C16–C22	3.431(12)
(b)	S3–C5	3.456(9)
	S4–C6	3.550(8)
	S4–C7	3.509(9)
	C11–C19	3.475(15)
	C12–C18	3.470(13)
	C13–C17	3.456(12)
	C14–C16	3.441(12)
	C15–C15	3.408(12)
(c)	C24–N36	3.333(10)
	C25–C31	3.474(10)
	C26–C30	3.320(10)
(d)	d_1	3.38
	d_2	3.26
	d_3	3.084(9)
	d_4	3.252(7)

Fig. 5.   ORTEP drawing of TTF (a) and OCNAQ (b) in TTF–OCNAQ(II) showing the atom numbering scheme.

Table 5.   Atomic Parameter of TTF–OCNAQ(II) ($\times 10^4$)

	x	y	z	$B_{eq}(\text{Å}^2)$
S1	−3650(5)	1130(2)	7841(5)	4.1
S2	727(5)	1557(2)	8228(5)	3.8
S3	−2770(5)	−453(2)	7189(5)	3.4
S4	1624(5)	−25(2)	7597(5)	3.5
C5	−2805(20)	1979(6)	8431(19)	4.4
C6	−841(21)	2173(6)	8613(19)	4.6
C7	−1171(17)	883(6)	7839(16)	3.0
C8	−858(18)	196(6)	7559(15)	2.9
C9	−1140(19)	−1077(6)	6902(17)	3.8
C10	809(19)	−884(6)	7112(17)	3.8
N11	−3420(16)	6940(5)	1348(17)	5.1
N12	−9303(15)	5894(6)	330(16)	5.2
N13	−4643(16)	2036(5)	2940(16)	4.8
N14	1591(16)	2739(5)	4124(19)	5.8
C15	−4380(16)	5166(5)	2792(15)	2.4
C16	−5763(16)	4559(5)	2560(15)	2.6
C17	−4987(17)	3914(6)	3063(16)	3.0
C18	−2801(17)	3790(5)	3732(15)	2.6
C19	−1362(16)	4403(5)	4360(15)	2.2
C20	−2167(16)	5087(5)	3844(14)	2.2
C21	−725(17)	5652(5)	4537(16)	2.6
C22	−5274(16)	5791(6)	1902(16)	2.9
C23	−4200(17)	6415(5)	1621(17)	3.2
C24	−7528(18)	5833(6)	1034(16)	3.4
C25	−2148(17)	3111(5)	3736(17)	2.9
C26	−3603(19)	2532(6)	3289(18)	3.6
C27	−50(20)	2933(6)	3951(19)	3.7

two kinds of interplanar spacings between the TTT molecules. Spacing between A and B (3.26 Å; d_2 in Fig. 3) is shorter than that between B and A' (3.38 Å; d_1 in Fig. 3) by 0.12 Å. The molecular overlapping pattern between A and B is the same as that observed in TTT$_2$I$_3$,[8] and there are short contacts between sulfur atoms (3.506(3) Å). On the other hand the molecular overlapping between B and A' is not the same as the pattern reported so far, and there are no effective S···S contacts (>3.9 Å). Consequently, TTT is weakly dimerized between A and B in the stack. As can be seen from Fig. 4(c), the overlap between the OCNAQ molecules is only partial; therefore, the interaction is supposed to be weak. The shortest contact between OCNAQ molecules (3.33(1) Å) are actually larger than those observed in Et$_4$N·OCNAQ (3.05(1) and 3.14(1) Å).[2] Interestingly, a rather strong interaction of OCNAQ exists in the direction toward the donor molecules. As shown in Fig. 3, two nitrogen atoms of OCNAQ strongly interact with the sulfur atoms of TTT. The distances of d_3 (3.084(9) Å) and d_4 (3.252(7) Å) are less than the sum of the van der Waals radii, 3.35 Å. Consequently, the interactions between the molecules in this system are rather two-dimensional.

TTF-OCNAQ(II): The molecular structures of TTF and OCNAQ in this compound are shown in Fig. 5, and the atomic parameters are listed in Table 5.[7] The TTF molecule is perfectly planar (deviations from the mean plane are less than 0.05 Å for the non-hydrogen atoms). The structure of OCNAQ is practi-
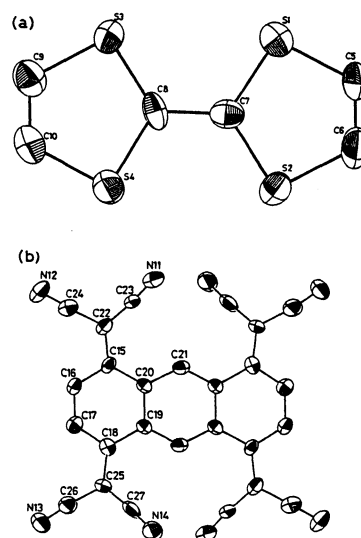
cally the same as that in TTT–OCNAQ(II). As listed in Table 3 the bond lengths of OCNAQ are close to the values observed for OCNAQ⁻. The mean dimensions of TTF (Table 6) are closer to those observed in TTF–TCNQ, in which the oxidation state of TTF is +0.59, than those of TTF⁰. Therefore, the electronic structure of this complex is supposed to be near (TTF)$^{\frac{1}{2}}$OCNAQ⁻, although there remains some ambiguity (vide infra).

Table 6.   Mean Dimensions of TTF (Å)

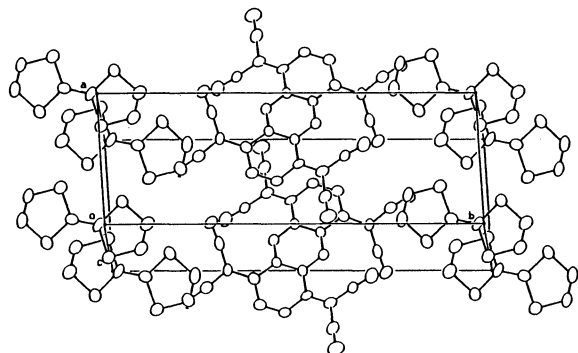|	TTF[a)	TTF-TCNQ[b)	TTF-OCNAQ(II)
J	1.349(3)	1.372(4)	1.392(16)
K	1.757(2)	1.745(3)	1.730(16)
L	1.726(2)	1.739(3)	1.733(13)
M	1.314(3)	1.326(4)	1.305(19)

a) Ref. 11. b) Ref. 12.

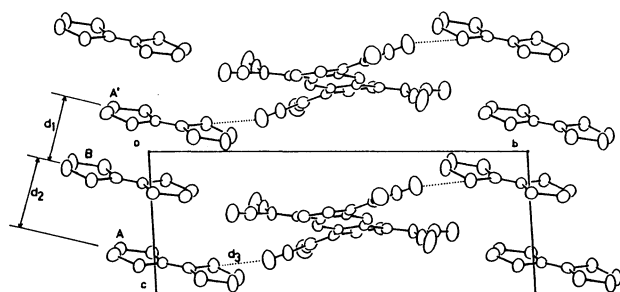Fig. 6.   Crystal structure of TTF-OCNAQ(II).

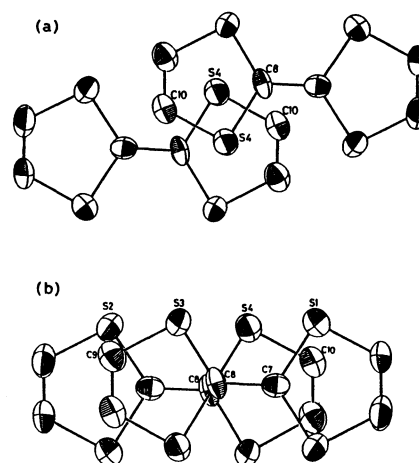Fig. 7.   Donor and acceptor arrangement in TTF-OCNAQ(II) in the (100) plane.

Fig. 8.   Molecular overlapping between the TTF molecules; between A and B (a), and between B and A′ (b) in Fig. 7.
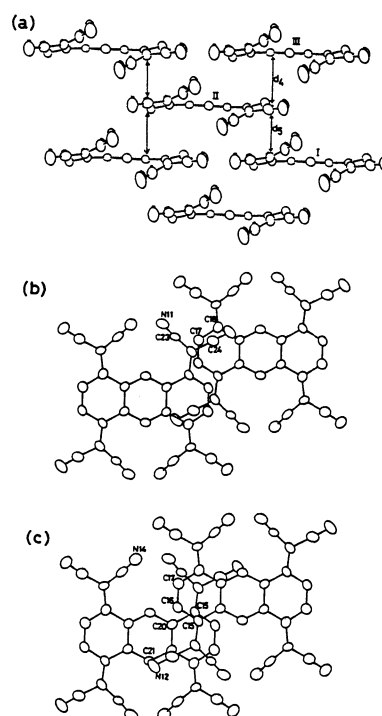

Fig. 9.   Molecular overlapping between the OCNAQ molecules; side view of the OCNAQ stack (a), between I and II (b), and between II and III (c) in (a).

The crystal structure is shown in Figs. 6 and 7. The TTF molecule forms one-dimensional columns along the c-axis, and there are no effective intermolecular contacts between the columns. Molecular overlapping patterns between the TTF molecules and between the OCNAQ molecules are shown in Figs. 8 and 9, respectively, and the interplanar and interatomic distances are listed in Table 7. The overlapping pattern between the TTF molecules of B and A′ is similar to that of TTF-TCNQ.[12] in which the intermolecular S⋯S distances are rather large (>3.70 Å). On the other hand, in the overlapping pattern between A and B there is a shorter S⋯S contact (S4⋯S4; 3.671(5) Å). However, this distance is still longer than those observed for the eclipsed-type stacking of TTF in TTF·X_y (3.55—3.60 Å; where X=Cl, Br, I, and etc.).[13]

In contrast with the case of TTT-OCNAQ(II), efficient stacking of OCNAQ in TTF-OCNAQ(II) can be seen from Fig. 6. There are two kinds of overlapping

patterns and one OCNAQ moleoule interacts with four OCNAQ molecules (Fig. 9). The interplanar distances listed in Table 7 are the distances between the mean planes, calculated for the anthracene framework. Although one of the interplanar distances is large (3.82 Å vs. 3.30 Å), the cyano groups, which are largely deviated from the plane, make the interatomic distances short (e.g., 3.345(17) Å for C17⋯C23). Therefore, the OCNAQ molecules effectively form a two-dimensional network in the (010) plane. In similarity to the TTT-OCNAQ(II) system, an extra interaction between nitrogen atoms of OCNAQ and a sulfur atom

Table 7. Interplanar and Interatomic Distances (Å) of TTF–OCNAQ(II); between A and B (a) and between B and A' (b) in Fig. 8, between I and II (c) and between II and III (d) in Fig. 9, and Distances Shown in Figs. 7 and 9 (e)

(a)	S4–S4	3.671(5)
	S4–C8	3.628(12)
	S4–C10	3.657(12)
	C8–C10	3.571(17)
(b)	S1–S4	3.717(6)
	S2–S3	3.740(5)
	S3–S4	3.754(5)
	S1–C10	3.540(12)
	S2–C9	3.518(13)
	C7–C10	3.582(17)
	C8–C8	3.393(15)
(c)	N11–C17	3.492(16)
	C17–C23	3.345(17)
	C18–C24	3.560(17)
(d)	N12–C21	3.478(18)
	N14–C17	3.360(16)
	C15–C15	3.573(17)
	C15–C16	3.406(16)
	C16–C20	3.446(17)
(e)	d_1	3.42
	d_2	3.38
	d_3	3.292(11)
	d_4	3.30
	d_5	3.82

Fig. 10. Electrical resistivities of the OCNAQ complexes.

Fig. 11. Thermoelectric power of the OCNAQ complexes.

of TTF exists. However, the distance, 3.292(11) Å, is not as short as those observed in TTT–OCNAQ(II).

Charge Transport. The electrical resistivities of the OCNAQ complexes are shown in Fig. 10, except for pyrene–OCNAQ and PT–OCNAQ, which are electrically insulating. The data shown in Fig. 10 were obtained along the long axis of the crystal.

TMTTF–OCNAQ and TTF–OCNAQ(I): As revealed by the infrared spectra, TMTTF–OCNAQ and TTF–OCNAQ(I) are simple salts. The temperature dependence of the resistivities shows a semiconducting behavior with activation energies of 0.14 eV for TMTTF–OCNAQ and 0.15 eV for TTF–OCNAQ-(I). The resistivities at room temperature, 10^2—10^3 Ω cm, are rather small compared with those of usual simple radical salts. This supposedly reflects the main effect produced by the twin-type structure, i.e., a reduced on-site Coulomb repulsion. Indeed, the resistivity at room temperature of $Et_4N \cdot OCNAQ$ is of the same order $(2.5 \times 10^3 \text{ Ω cm})$.[2)]

The thermoelectric power (TEP) data are shown in Fig. 11. For a simple salt the energy gap is usually related to the on-site Coulomb repulsion. In these systems the on-site Coulomb repulsion of a donor molecule is much larger than that of OCNAQ, and the charge transport of these systems should be largely governed by OCNAQ. The observed large negative values are consistent with electron conduction through OCNAQ.
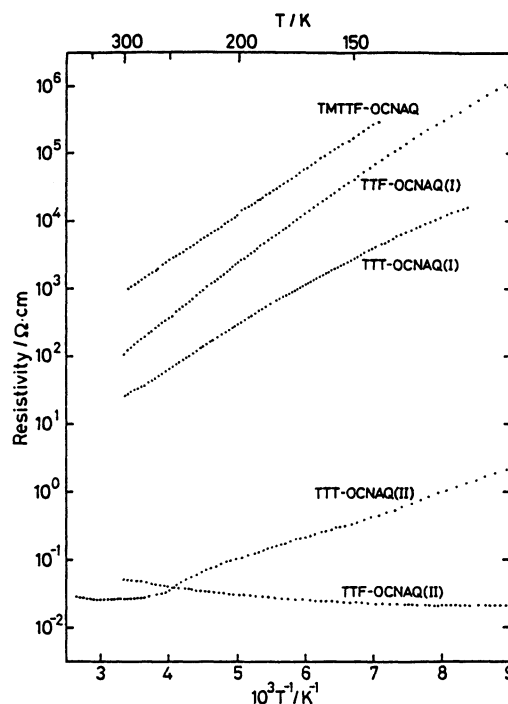
TTT–OCNAQ(I): Since the electronic structure of

this complex is $(TTT_3)^{+2}(OCNAQ^-)_2$(dichlorobenzene)$_2$, the TTT molecule is formally charged by +2/3. Thus, the resistivity of this compound is expected to be lower than those of simple salts. In fact the resistivity is lower compared with TMTTF–OCNAQ and TTF–OCNAQ(I), although the temperature dependence is semiconducting (Fig. 10). The TEP data shown in Fig. 11 are consistent with TTT based hole conduction. In this compound OCNAQ simply acts as a

counterion, and makes no contribution to the charge transport.

TTT-OCNAQ(II): This compound shows a weak metallic behavior down to 250 K, at which point the material turns to the semiconducting state with an activation energy of 0.05 eV. As suggested by the structure analysis, there is a transverse interaction between the TTT columns through the OCNAQ molecules. In order to see this structural peculiarity the conduction was measured not only along the TTT stacking direction but also in the direction corresponding to the transverse interaction. The results are shown in Fig. 12. The anisotropy of the conduction, $\rho(\perp c)/\rho(//c)$, was found to be 30. This value is the smallest among the TTT complexes so far reported.

The TEP measurements were also carried out for both directions, and the results are shown in Fig. 13. The TEP is linearly correlated to the temperature in both directions above 250 K, which corresponds to the metallic state of this compound observed by the con-
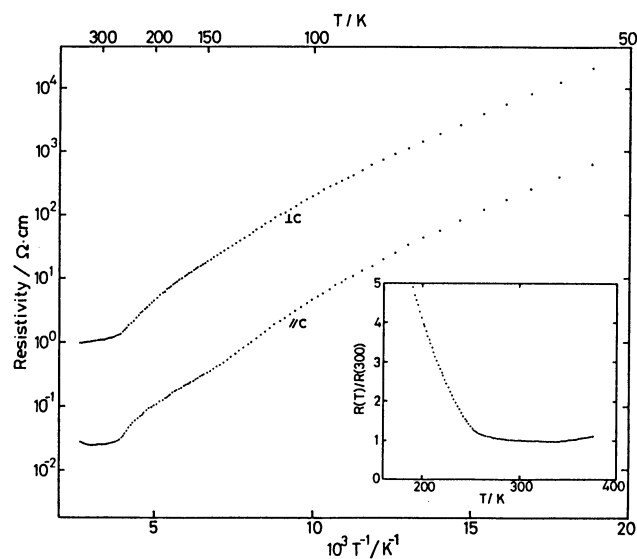

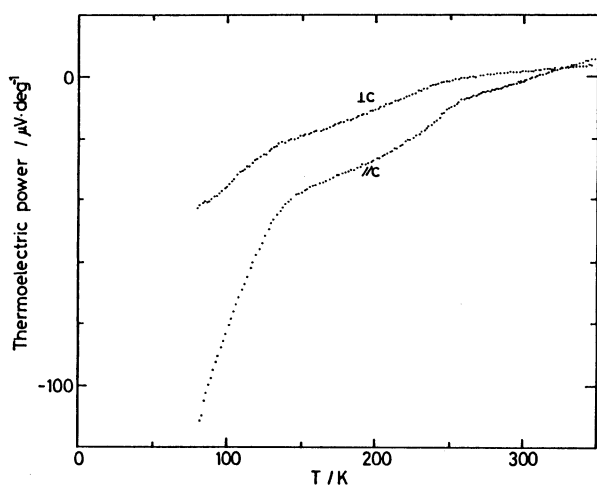Fig. 12. Electrical resistivities of TTT-OCNAQ(II).

Fig. 13. Thermoelectric power of TTT-OCNAQ(II).

duction measurements. The positive slope suggests that the major charge carrier is a hole in the TTT stacks. However, the TEP crosses zero in the metallic region and becomes negative below the anomaly at 250 K. This behavior is not a typical one of low-dimensional radical cation salt-type conductors, such as D_2X, where D is a donor and X is a counterion, in which the conduction occurs only through the donor stacks. In such compounds the TEP usually decreases towards zero in the metallic region. The deviation from the typical behavior in TTT-OCNAQ(II) is, thus, caused by the structural peculiarity of this compound, i.e., the existence of a transverse interaction between the TTT columns through OCNAQ. When the interaction between the TTT molecules in the stack is large, the total interaction between the donor and acceptor molecules in the system is nearly two-dimensional in the $(\bar{1}10)$ plane. However, even at room temperature the TTT molecules are not stacked uniformly, and are weakly dimerized between molecules A and B in Fig. 3. If the dimerization of TTT becomes more developed with decreasing temperature, an energy gap is opened along the stacking direction. However, the interaction along the [112] direction, which corresponds to the $(TTT)_2 \cdots OCNAQ \cdots (TTT)_2$ chain, will remain. The charge transport along this chain below 250 K is supposed to be governed by OCNAQ, since the sign of TEP is changed. The additional anomaly at 140 K, which is detectable in the resistivity data, may be related to this chain.

The structure of this compound has some similarities to HMTSF-TCNQ,[14] where HMTSF is bis(trimethylene)tetraselenafulvalene, in which short Se$\cdots$N contacts between the donor and acceptor molecules exist. The anisotropy of conduction of this material is also 30. The most remarkable characteristic of this material is that the metallic state is stabilized at very low temperature. Comparing this system to TTT-OCNAQ(II), two structural differences can be noted. First, the interaction between the acceptor molecules: in HMTSF-TCNQ a rather strong interaction between the TCNQ molecules exists, while in TTT-OCNAQ(II) the interaction between the OCNAQ molecules is quite weak. Secondly, the pattern of the interaction between the donor and acceptor molecules is different. In HMTSF-TCNQ all the nitrogen atoms of TCNQ interact with all the selenium atoms of HMTSF so that a uniform stacking of the donor (acceptor) is maintained by the transverse interaction with the neighboring acceptor (donor) stacks. On the other hand, in TTT-OCNAQ(II) only two of the eight nitrogen atoms of OCNAQ interact with two of the four sulfur atoms of TTT. This type of transverse interaction is not sufficient to prevent the deformation of the donor stack. These structural differences may cause the difference in the physical properties.

TTF-OCNAQ(II): The temperature dependence of the conductivity is shown in Fig. 14. The conduc-

tivity increases with decreasing temperature down to ca. 90 K then gradually decreases; at 43 K, where the conductivity is still as high as that observed at room temperature, a sharp drop occurs. The temperature dependence of the TEP is shown in Fig. 15. The TEP decreases linearly down to 90 K, and then starts to increase. If this anomaly is due to a metal-to-insulator transition, this upturn is assumed to be caused by a gap formation of the donor stack. However, the TEP below 90 K does not fit a simple activation behavior. Furthermore, for simple hole conduction the zero crossing at 160 K cannot be explained. The TEP rather increases linearly towards zero. This means that the charge transport is metallic and that the major charge carrier is an electron in this region. As discussed in the structure analysis, a crystal of this material consists of TTF and OCNAQ stacks. Thus, the major route of conduction is the TTF stacks above 90 K; it changes to OCNAQ stacks in the region between

Fig. 14.   Electrical conductivity of TTF–OCNAQ(II).

Fig. 15.   Thermoelectric power of TTF–OCNAQ(II).

43 and 90 K. The material is essentially in a semimetal state. The anomaly at 43 K is assumed to be a normal metal-to-insulator transition.

It is noteworthy that conduction through the OCNAQ stacks is realized in this system. This fact suggests that the reduction state of OCNAQ is slightly deviated from an integral value. Such a fractional charge is stabilized only if considerable electron transfer interaction between molecules exists. Although the OCNAQ molecule is not planar, the existence of an intermolecular interaction between the OCNAQ molecules is indicated by an X-ray structure analysis, and the charge transport properties of this material strongly suggests that the interaction is sufficient enough to stabilize the metallic character of the OCNAQ stacks.

Remarks

In the present paper various aspects of OCNAQ are reported. The reduced on-site Coulomb repulsion is manifested in the electrical properties of simple salts. In TTT–OCNAQ(II) a unique transverse interaction through OCNAQ molecules has been found. In TTF–OCNAQ(II) the metallic character of OCNAQ stacks has been observed. Of further interest is the stacking pattern of the OCNAQ molecules in TTF–OCNAQ-(II), in which one OCNAQ undergoes interactions with four OCNAQ molecules. Therefore, this interaction is completely two-dimensional. This stacking pattern is the type expected for a molecule having a twin-type structure. Unfortunately, in this system the stabilization of the metallic state at low temperatures is not realized, since the transfer integral is not sufficiently large to maintain the metallic nature at low temperatures, due to the nonplanarity of the molecule. However, it should be pointed out that one promising approach to design two-dimensional systems is to use such twin-type donor or acceptor molecules.

References

1)   T. Mitsuhashi, M. Goto, K. Honda, Y. Maruyama, T. Sugawara, T. Inabe, and T. Watanabe, *J. Chem. Soc., Chem. Commun.*, **1987**, 810.

2)   T. Mitsuhashi, M. Goto, K. Honda, Y. Maruyama, T. Inabe, T. Sugawara, and T. Watanabe, *Bull. Chem. Soc. Jpn.*, **61**, 261 (1988).

3)   T. Inabe, T. Mitsuhashi, and Y. Maruyama, *Chem. Lett.*, **1988**, 429.

4)   P. M. Chaikin and J. F. Kwak, *Rev. Sci. Instrum.*, **46**, 218 (1975).

5)   T. Sakurai and K. Kobayashi, *Rep. Inst. Phys. Chem. Res.*, **55**, 69 (1979).

6)   J. S. Chapell, A. N. Bloch, W. A. Bryden, M. Maxfield, T. O. Poehler, and D. O. Cowan, *J. Am. Chem. Soc.*, **103**,
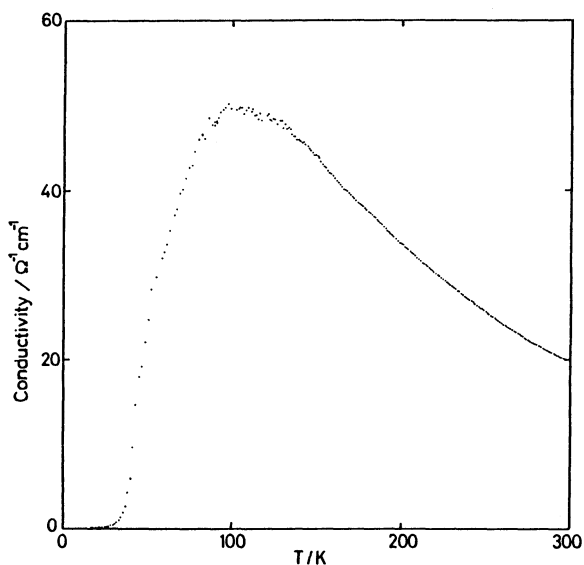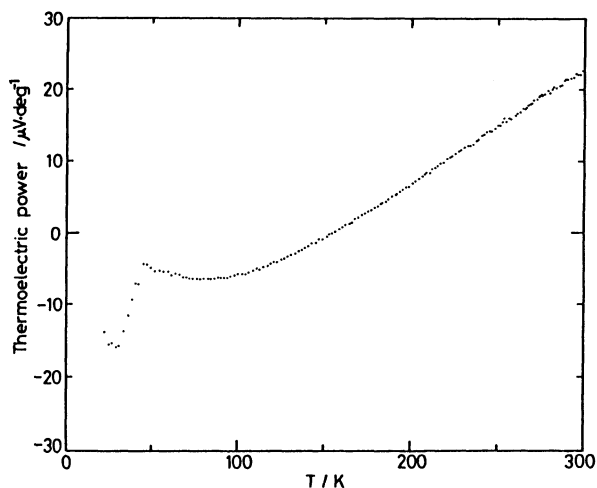
2442 (1981).

7) The lists of structure factors, atomic parameters for hydrogen atoms, and anisotropic thermal parameters for non-hydrogen atoms are deposited at Bull. Chem. Soc. Jpn. (Document No. 8843).

8) D. L. Smith and H. R. Luss, *Acta Crystallogr., Sect. B,* **33,** 1744 (1977).

9) O. Dideberg and J. Toussaint, *Acta Crystallogr., Sect. B,* **30,** 2481 (1974).

10) R. P. Shibaeva and L. P. Rozenberg, *Sov. Phys. Crystallogr.,* **20,** 581 (1976).

11) W. F. Cooper, N. C. Kenney, J. W. Edmonds, A. Nagel, F. Wudl, and P. Coppens, *Chem. Commun.,* **1971,**

889.

12) T. J. Kistenmacher, T. E. Phillips, and D. O. Cowan, *Acta Crystallogr., Sect. B,* **30,** 763 (1974).

13) C. K. Johnson and C. R. Watson, Jr., *J. Chem. Phys.,* **64,** 2271 (1976); B. A. Scott, S. J. Laplaca, J. B. Torrance, B. D. Silverman, and B. Welber, *J. Am. Chem. Soc.,* **99,** 6631 (1977).

14) J. R. Cooper, M. Weger, D. Jerome, D. Lefur, K. Bechgaard, A. N. Bloch, and D. O. Cowan, *Solid State Commun.,* **19,** 749 (1976).

15) C. K. Johnson, ORTEP, Report ORNL-3794, Oak Ridge National Laboratory, Tennessee (1976).